CLEMENTI, E., ROOTHAAN, C. C. J. & YOSHIMINE, M. (1962). *Phys. Rev.* **127**, 1618.
COOPER, M., LEAKE, J. A. & WEISS, R. J. (1965). *Phil. Mag.* **12**, 797.
COOPER, M. & LEAKE, J. A. (1966). *Phil. Mag.* **13**, 603.
CORNILLE, M. (1963). Private communication.
CORNILLE, M. (1966). To be published.
COWAN, R. D., LARSON, A. C., LIBERMAN, D., MANN, J. B. & WABER, J. B. (1966). *Phys. Rev.* **144**, 5.
DAWSON, B. (1961). *Acta Cryst.* **14**, 1117.
DONATH, W. E. (1961). *J. Chem. Phys.* **35**, 817.
DUMOND, J. W. M. (1933). *Rev. Mod. Phys.* **5**, 1.
DUNCANSON, W. E. & COULSON, C. A. (1944). *Proc. Roy. Soc.* A, **62**, 37.
IBERS, J. A. (1958). *Acta Cryst.* **11**, 178.
IIJIMA, T., BONHAM, R. A. & ANDO, T. (1963). *J. Phys. Chem.* **67**, 1472.
KILBY, G. E. (1963). Thesis, Sheffield Univ.
KILBY, G. E. (1965). *Proc. Phys. Soc. London*, **86**, 1037.
MOCCIA, R. (1964). *J. Chem. Phys.* **40**, 2164, 2176, 2186.
MORSE, P. M. (1932). *Phys. Z.* **33**, 343.
RANSIL, B. J. (1966). To be published.
ROOTHAAN, C. C. J. (1951). *J. Chem. Phys.* **19**, 445.
ROSENFELD, J. L. J. (1964). *Acta Chem. Scand.* **18**, 1719.
ROUAULT, M. & GERVAIS, A. (1966). Private communication (preliminary results).
ROBINSON, D. W. (1965). *J. Phys. Chem.* **69**, 3357.
SACHS, L. M. (1961). *Phys. Rev.* **124**, 1283.
SEARS, F. W. (1959). *An Introduction to Thermodynamics: The Kinetic Theory of Gases, and Statistical Mechanics.* 2nd ed., p.236. Reading, Mass.: Addison-Wesley.
SLATER, J. C. (1930). *Phys. Rev.* **36**, 57.
SMITH, P. R. & RICHARDSON, J. W. (1965). *J. Phys. Chem.* **69**, 3346.
TAVARD, C. (1966). Thèse de Doctorat, Orsay, France.
TAVARD, C. & ROUX, M. (1965). *C. R. Acad. Sci. Paris*, **260**, 4460, 4933.
TAVARD, C., ROUX, M. & CORNILLE, M. (1962). *C. R. Acad. Sci. Paris*, **255**, 3386.
TAVARD, C., ROUX, M. & CORNILLE, M. (1963). *J. Chem. Phys.* **39**, 2390.
TAVARD, C., ROUX, M. & ROUAULT, M. (1964). *J. Chem. Phys.* **41**, 1324, 1330.
TONG, B. Y. & SHAM, L. J. (1966). *Phys. Rev.* **144**, 1.
TSAPLINE, B. (1966). Thèse de 3ème cycle, Paris.
WALLER, I. & HARTREE, R. D. (1929). *Proc. Roy. Soc.* A, **124**, 119.

Acta Cryst. (1967). **22**, 639

The Structure of Potassium Niobate at Room Temperature: The Solution of a Pseudosymmetric Structure by Fourier Methods

BY LEWIS KATZ* AND HELEN D. MEGAW
Crystallographic Laboratory, Cavendish Laboratory, Cambridge, England

(*Received* 5 *September* 1966)

In principle, the refinement of a pseudosymmetric structure starting from an idealized high-symmetry structure is impossible by routine methods of analysis, such as least-squares, even when the atomic displacements are very small. A much more helpful approach is by a method of successive approximations. This uses first the most important displacement parameters, whose magnitudes (but not signs) can be estimated from electron-density maps or difference maps based on the ideal structure. Certain of their signs can be allotted arbitrarily, and the further analysis follows step by step until a realistic trial model is obtained in which all (or at least a large proportion of) the displacement parameters have the correct and consistent signs and very roughly correct magnitudes. At this stage, routine use of least-squares refinement becomes permissible.

This method has been applied successfully to $KNbO_3$ at room temperature, using X-ray diffraction data. The structure is strictly isomorphous with orthorhombic $BaTiO_3$, with space group *Bmm*2 and 1 formula-unit per cell, but all deviations from the perovskite aristotype are rather larger in $KNbO_3$. The NbO_6 octahedra are nearly regular, with Nb displaced by 0·17 Å from their centres, giving Nb–O bond lengths of 1·86, 1·99, and 2·18 Å. Since all the octahedra are parallel, the crystal is ferroelectric.

Comparison of $KNbO_3$ with $BaTiO_3$ directs attention to the importance of O–O repulsions in the octahedron edges. By treating nearest-neighbour contacts as a system of links in a state of compression or tension, and applying simple statics, a consistent though qualitative explanation can be given of all the differences, in terms of the difference in Nb–O and Ti–O bond lengths on the one hand, in size and polarizability of K and Ba on the other; the structural features attributable to each of these causes can be distinguished.

Introduction

Potassium niobate, $KNbO_3$, has a structure belonging to the perovskite family. It is polymorphous, and isomorphous in all its forms with barium titanate, though the corresponding transition temperatures are higher for potassium niobate. Their ferroelectric properties are also closely similar. The present work is concerned with the orthorhombic form, stable at room temperature. The general character of the structure has been known for a good many years; the determination

* Work done during leave of absence from the Department of Chemistry, University of Connecticut, Storrs, Connecticut, U.S.A.

of the atomic parameters remained to be done, and is the subject of the present work.

In view of the discussions there have been about barium titanate concerning the difficulties of this type of structure (Evans, 1961; Geller, 1961; Megaw, 1962), the steps involved in the Fourier methods adopted here were examined rather carefully, and some account of the important points is given below. As a result of the structure analysis, it was found that physically meaningful values could be obtained both for position parameters and for thermal parameters, and that limits of error could be estimated. The precision of the parameters, though not as good as might have been achieved with more elaborate experimental work, allows a useful description of the structure to be given, with sufficient accuracy for most purposes.

Unit cell and space group

It was shown by Wood (1951) that room-temperature $KNbO_3$ is orthorhombic, and that two symmetry axes (here called x and z) lie along the cube face diagonals of the aristotype*, giving a unit cell of approximately $5{\cdot}6 \times 4 \times 5{\cdot}6$ Å, which is face-centred on B. Since the material is ferroelectric, the point group is polar, and is therefore $\{mm2\}$ (the curly brackets indicating that the axial directions implied in this symbol have not yet been matched to those chosen for the description of the crystal). Since there is only one formula unit per lattice point in the hettotype* as in the aristotype, both Nb and K must lie on special positions, which, in this point group, can only be the intersections of two mirror planes, coinciding with a rotation axis – the polar axis. It remains to determine the direction of this axis relative to the unit cell. Most workers have apparently assumed, from the close analogy with orthorhombic $BaTiO_3$, that the space group is the same, and that the polar axis is the long diagonal of the rhombus corresponding to a cube face. We have been unable to find any report of experimental work explicitly confirming these assumptions, but the present work does so, as explained in a later section. If the long diagonal of the rhombus is called z, the space group is then $Bmm2$.

Both the choice of origin on z and the choice of sense of z are arbitrary. Taking the origin at Nb, the atomic coordinates are:

Nb	$0,0,0$
K	$0,\frac{1}{2},\frac{1}{2}+z_K$
O(1)	$0,\frac{1}{2},z_1$
O(2)	$\frac{1}{4}+x_2,0,\frac{1}{4}+z_2$

The sense of displacement of K may arbitrarily be taken as positive. Since the *displacement parameters* z_K, z_1, z_2, and x_2 are all small the structure is already known qualitatively; it remains to find their detailed values.

* The *aristotype* (αριστος, best) is in this case the ideal perovskite structure; a *hettotype* (ήττος, less good) is any of the lower-symmetry but topologically similar variants.

Principles of refinement

The difficulty of a detailed study of this structure arises from its pseudosymmetric character. Automatic refinement procedures cannot legitimately take the aristotype as a starting point, because they cannot generate displacements which lower the symmetry; moreover, the basic assumption underlying such procedures, that the structure factors vary linearly with position parameters throughout the range examined, is certainly not valid when the range includes special values. A different approach is needed.

Because of the heavy atom at a point which can be chosen as origin, the real parts of all (or nearly all) structure factors are large and positive, and the measured $|F|$'s are a good approximation to them. Since the real part of F is the average of F and its complex conjugate, the electron density obtained from a synthesis of the real parts, or of the measured $|F|$'s, is the average of the electron densities of the true structure and its image by inversion through a centre of symmetry at the origin. The map so obtained therefore represents a centrosymmetric structure where the displaced atoms of the true structure are replaced by centrosymmetric pairs of half-atoms with displacement parameters of the same magnitude. This map allows the magnitudes of the displacement parameters to be estimated but not their signs.

The signs cannot be found as long as a centrosymmetric model is used, because this gives only real F's and therefore prohibits any refinement of phase angles, while all information about displacement signs is contained in the imaginary part of the F_{obs}'s. For a start, one displacement parameter must be given an arbitrary sign. If the parameter chosen belongs to the second heaviest atom, and has a reasonably large magnitude, its contribution to the imaginary part of the F's will be sufficient to allow a useful approximation to the phase angles. A synthesis using the measured $|F|$'s with these first phase angles may, by emphasizing one half-atom of each pair at the expense of the other, allow the true structure to be picked out; or, if the approximation is still too rough, it may at least indicate the displacement sign for one other atom, and thus allow an improved approximation as the next step. Only when all displacement signs are clearly established (unless perhaps for a few displacements very much smaller than the rest) is automatic refinement a safe procedure.

In the early stages of sign determination, the reflexions which give most information are just those which do not satisfy the conditions for a good half-atom approximation, namely those where the real part of F is relatively small. Preferential use of evidence from classes of reflexions where this is systematically true may be a help. In the present work, no deliberate weighting of reflexions was done, but comparison of effects from the $(h0l)$ and $(h1l)$ layers, discussed below, illustrates the point.

There is a real danger, unless one is on the watch for it, that signs of displacements may be wrongly deduced from small indications which are in fact only random error. An example occurred in the present work, and is described in a later section. If it were not for this effect of random error (perhaps in some cases rounding-off error) the impossibility of automatic refinements from the centrosymmetric model would be obvious. Where no displacement parameter is deliberately given a sign, the refinement procedure *must* rely on random error to provide one and may equally readily accept inconsistent signs for several displacements at the same time. Similar troubles are likely when the parameter to which an arbitrary sign is allotted initially is given a trial magnitude much less than its true value. Once incorrect signs have been accepted, it is hard for the later stages of refinement to alter them. Thus a scrutiny of the steps taken to establish a suitable trial structure before automatic refinement begins is a much more searching test of reliability of the final structure than is a routine assessment of the errors of the latter by statistical methods.

The correct stage for beginning the refinement of thermal parameters is also important. It is not legitimate to allow them to increase (above the rather small values expected for normal atoms in chemically similar compounds) until the displacement parameters are known both in sign and in approximate magnitude. The greater the displacement parameters, the less the relative sensitivity of the calculated $|F|$'s to the corresponding thermal parameters. Hence correlation between displacement and thermal parameters is greatest for trial structures with very small displacements, and if both are allowed to refine together from a trial model unnecessarily close to the aristotype, an increase in the thermal parameter may do duty as substitute for the increase in displacement, whose refinement will therefore be slowed down and perhaps obscured altogether, whereas with a better trial structure the distinction might be quite obvious. This need for delay before allowing any increase in the isotropic thermal parameters applies even more strongly to the introduction of anisotropic thermal parameters.

The question of anisotropic thermal parameters is relevant to the interpretation of the half-atom map. If a displacement is small, the pair of half-atoms may not be resolved, and its elliptical peak may not be distinguishable analytically from a single anisotropic atom at the centre. This does not matter, because the half-atom map is only being used as a step towards the deduction of the single-displaced-atom map, and it is the difference between the latter and the centrosymmetric anisotropic atom which has to be considered. If the displaced-atom model is a clear improvement on the half-atom model, it is thereby an improvement on the anisotropic-atom model; if the postulated displacement is wrong, the centrosymmetric feature on the difference map will not refine away, and the model must be reconsidered. The introduction of thermal anisotropy before displacement signs are known thus prevents further progress; the initial assumption of small isotropic thermal parameters allows a model to be set up, after which the restriction can be relaxed.

Experimental work and refinement procedures

The crystal used was from a batch kindly provided by Dr E. A. Wood; it was a prism of form {101} elongated parallel to [010], approximately $0{\cdot}01 \times 0{\cdot}01 \times 0{\cdot}04$ cm in dimensions.

Cell dimensions were measured by the method of Farquhar & Lipson (1946). The values, $a = 5{\cdot}697$, $b = 3{\cdot}971$, $c = 5{\cdot}721$ Å, agreed to within about 0·001 Å with those of Vousden (1951) and Shirane, Newnham & Pepinsky (1954).

Weissenberg photographs of layers *h*0*l* to *h*3*l* were taken with Zr-filtered Mo $K\alpha$ radiation, using the multiple-film technique; intensities were measured visually and corrected for Lorentz and polarization effects and for absorption. This work (as well as the measurement of cell dimensions) was done by Dr R. Ueda, during a visit to Cambridge, and there was unfortunately no opportunity to supplement the data then or later by further observations, as would obviously have been desirable had time permitted. Since useful conclusions can be drawn from the existing evidence, in spite of its limited quantity, it seemed preferable to publish it rather than wait indefinitely for a chance to achieve greater precision.

In the refinement, atomic scattering factors for K and O were based on those of Berghuis and co-workers, for Nb on those of Thomas & Umeda (1957). Modifications for the state of ionization were made by joining the value for O^{2-} at the origin smoothly to the curve for neutral O at $(\sin\theta)/\lambda = 0{\cdot}2$, and the value for Nb^{5+} at the origin smoothly to the curve for Nb^{4+} at $(\sin\theta)/\lambda = 0{\cdot}4$; a dispersion correction to the real part of the scattering factor (Dauben & Templeton, 1955) was made for Nb. The scattering factors so obtained were used for the least-squares refinement. For the Fourier refinement they were fitted by least squares to Forsyth–Wells functions. The refinement of difference Fouriers was carried out with a program written for EDSAC II by M. Wells. The first stage of the least-squares refinement used the Busing–Levy program and was done for us by R. Dobrott at Harvard with the kind permission of Professor W. N. Lipscomb; subsequent work was done at the University of Connecticut, and incorporated a dispersion correction to both real and imaginary parts.

Structure factors

The structure factors are all of the form

$$f_{\mathrm{Nb}} \pm f_{\mathrm{K}} \exp 2\pi i l z_{\mathrm{K}} \pm f_{\mathrm{O}} \exp 2\pi i l z_1 \pm 2 f_{\mathrm{O}} \exp 2\pi i l z_2 \begin{pmatrix}\cos\\ \sin\end{pmatrix} 2\pi h x ,$$

the signs, and the choice between cos or sin in the last term, depending on the conditions satisfied by *h*, *k*, *l*.

It is convenient to separate the real and imaginary parts; the coefficients of the different atomic scattering factors in these for the various classes of reflexions are given in Table 1. In the aristotype, all c's (cosine factors) are unity and all s's (sine factors) zero; in the actual structure, c's are generally nearly unity and s's small.

Study of the *h0l* projection

An electron density map was made from the observed $|F|$'s. This showed peaks elongated along the long axis, z.

This provides strong direct evidence for the direction of the polar axis in the structure. Only along the polar axis can there be displacement of atoms from special positions [except for O(2)]. Hence only in this direction can the half-atom map show doubled or elongated peaks due to displacements. On the map, the elongation of the K peak, which overlaps with no other atom, is quite unmistakable, and is parallel to the long diagonal of the rhomb. Even supposing the elongation were due to thermal anisotropy, if the long diagonal were not the polar axis it would mean that both thermal parameter and displacement parallel to the polar axis must be smaller than in other directions, which is improbable. A direct check was, however, made by taking a trial structure with the shorter diagonal as the polar axis; it gave worse agreement, and did not refine. In the literature, the two alternative definitions of axial direction **c** (or z) in terms of the polar axis or of the long diagonal of the rhomb have been used uncritically; the present work provides evidence that they are in fact consistent with each other.

The estimate of 0·0156 for z_K from this map, and the allocation of a positive sign to it, allowed phases to be calculated and a new map to be constructed. The same isotropic temperature factor was used for all atoms, with a value $B=0{\cdot}6$ Å^2 estimated from preliminary studies; tests with B_K assigned separate values ranging from 0 to 1·2 Å^2 showed no significant differences.

It had been clear from the first map that the next most important displacement was z_2; on the new map, the double peak indicated a magnitude of 0·023, and

Table 1. *Structure factors*

Types of indices			Coefficients of atomic scattering factors*				
				Real part		Imaginary part	
h and l	$h+l$	k	f_{Nb}	f_K	f_O	f_K	f_O
Even	$4n$	Even	1	$+cz_K$	$+cz_1+2cz_2cx_2$	$+sz_K$	$+sz_1+2sz_2cx_2$
Even	$4n$	Odd	1	$-cz_K$	$-cz_1+2cz_2cx_2$	$-sz_K$	$-sz_1+2sz_2cx_2$
Even	$4n+2$	Even	1	$+cz_K$	$+cz_1-2cz_2cx_2$	$+sz_K$	$+sz_1-2sz_2cx_2$
Even	$4n+2$	Odd	1	$-cz_K$	$-cz_1-2cz_2cx_2$	$-sz_K$	$-sz_1-2sz_2cx_2$
Odd	$4n$	Even	1	$-cz_K$	$+cz_1-2sz_2sx_2$	$-sz_K$	$+sz_1+2cz_2sx_2$
Odd	$4n$	Odd	1	$+cz_K$	$-cz_1-2sz_2sx_2$	$+sz_K$	$-sz_1+2cz_2sx_2$
Odd	$4n+2$	Even	1	$-cz_K$	$+cz_1+2sz_2sx_2$	$-sz_K$	$+sz_1-2cz_2sx_2$
Odd	$4n+2$	Odd	1	$+cz_K$	$-cz_1+2sz_2sx_2$	$+sz_K$	$-sz_1-2cz_2sx_2$

* Abbreviations used:

$cz=\cos 2\pi lz$, $sz=\sin 2\pi lz$

$cx=\cos 2\pi hx$, $sx=\sin 2\pi hx$

Table 2. *Displacement parameters and thermal parameters*

	(1) From *h0l*	(2) From *h1l*	(3) From *h0l*/*h1l*	(4) From Fourier 3-D	(5) From least-squares: oscillation extremes	Final mean and error
z_K	0·0148	0·0172	0·0160	0·0152	0·0164–0·0177	0·017 ± 0·001
z_1	—	—	(0·020)	0·0169	0·0193–0·0232	0·021 ± 0·002
z_2	0·0312	0·0364	0·0338	0·0337	0·0348–0·0350	0·035 ± 0·002
x_2	0·0017	0·0038	0·0028	0·0036	0·0037–0·0038	0·004 ± 0·002
					*	
B_{Nb}	0·55 Å^2	0·6 Å^2	—	0·52 Å^2	(11) 0·474 – 0·510 Å^2	0·49 ± 0·02 Å^2
					(33) 0·531 – 0·576	0·55 ± 0·02
B_K	0·75	1·0	—	0·95	(11) 0·749 – 0·780	0·76 ± 0·02
					(33) 0·667 – 0·726	0·70 ± 0·03
$B_{O(1)}$	0·85	1·0	—	0·69	(11) 0·620 – 0·734	0·68 ± 0·06
					(33) 1·110 – 1·611	1·36 ± 0·25
$B_{O(2)}$	0·85	1·0	—	0·89	(11) 0·779 – 0·886	0·83 ± 0·06
					(33) 0·813 – 1·010	0·95 ± 0·14
					(13) (−0·125) – (−0·216)	−0·17 ± 0·05

* The thermal parameters labelled (11), (33) and (13) are the quantities $4a^2\beta_{11}$, $4c^2\beta_{33}$, and $4ac\beta_{13}$, where $B(\sin\theta/\lambda)^2=\beta_{11}h^2+\beta_{22}k^2+\beta_{33}l^2+2\beta_{12}hk+2\beta_{13}hl+2\beta_{23}kl$.

As explained in the text, β_{22} can not be determined from the data; β_{12} and β_{23} are always zero, as is β_{13} for all atoms except (O2).

a slight enhancement of the peak in the direction indicating a negative sign was mistakenly accepted as significant. This peak also gave a small positive value for x_2. O(1) was too close to Nb to allow the determination of z_1, but the other parameters were refined for several cycles.

When the parameters so obtained were used to calculate F's for the higher layers, it became clear that something was wrong, because the R values were about 20% for layers 1 and 3 and only 9% for layers 0 and 2, though there were no gross systematic intensity differences between odd and even layers to account for it. Inspection showed that the trouble was most apparent for reflexions with h and l even, $\frac{1}{2}(h+l)$ odd and k odd. It can be seen from Table 1 that this class of reflexion has the systematically smallest real part, all contributions from atoms other than Nb being negative, and therefore it is most sensitive to the relative signs of z_K and z_2. On changing the sign of z_2, the R values for the odd layers dropped by about 6%.

Further refinement of $h0l$ difference maps gave the parameters shown in Table 2, column 1.

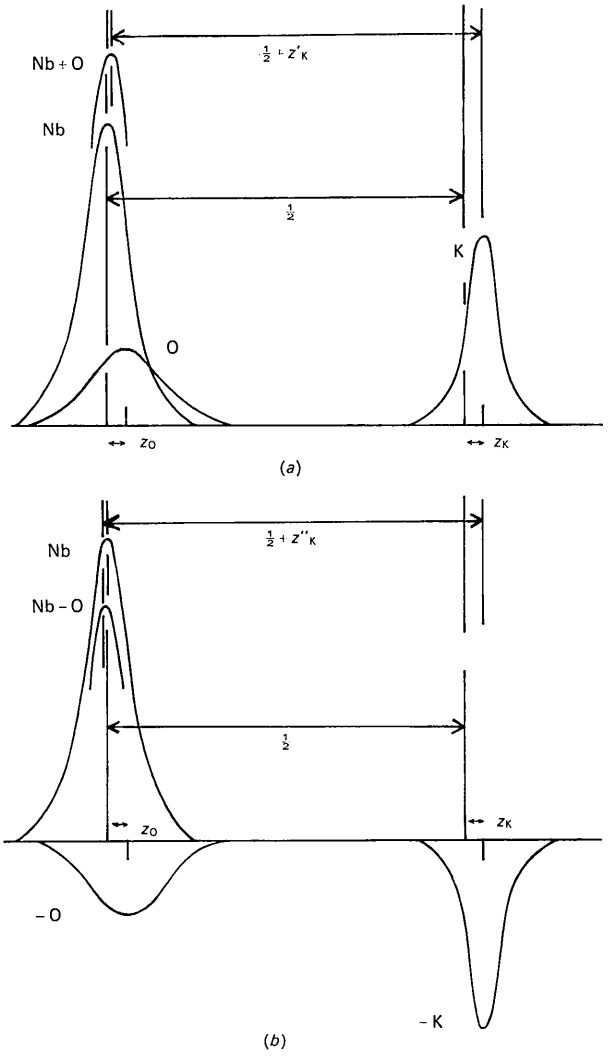

Fig. 1. Effect of Nb/O(1) overlap on measured displacement, (*a*) in $h0l$ projection, (*b*) in $h1l$ generalized projection.

h1l generalized projection

As a check, and to see what further information could be obtained, the same procedure was applied to the $h1l$ layer. For the first F_O map and difference map, z_K was set at the value obtained from $h0l$, all other displacements were made zero, and a single isotropic temperature factor was assumed. Very clear indications were given of a positive sign for z_2, and smaller indications of a positive sign for x_2. With z_1 still kept at zero, four further cycles of refinement led to the parameters of column 2 in Table 2.

The problem of atom O(1)

In the $h0l$ projection, O(1) is poorly resolved from Nb; together they form a composite peak whose maximum lies slightly on the O(1) side of Nb. Since the refinement procedure assumes that there is a large centrosymmetric peak at the origin, it measures position parameters from the maximum, which is most nearly centrosymmetric, rather than from Nb.

An estimate of the separation of Nb from the composite peak can be made by comparison of the values of z_K derived from $h0l$ and $h1l$, as illustrated in Fig. 1. In the $h1l$ map, the O(1) peak is negative, and therefore the composite maximum is on the side of Nb *remote* from O(1). Hence the true value of z_K lies between the values measured from $h0l$ and $h1l$, and an order-of-magnitude estimate of the Nb-peak displacement is given by half their difference. A similar argument holds for the two values of z_2. The estimates from z_K and z_2 are $-0{\cdot}0012$ and $-0{\cdot}0026$ respectively. They agree in their order of magnitude and in their negative sign. Since Nb is on the negative side of the peak, O(1) must be on the positive side. A rough estimate of its magnitude can be obtained on the assumption that the Nb and O(1) displacements from the maximum are in the inverse ratio of the Nb and O(2) peak heights. The value so obtained is given in brackets in column 3 of Table 2. In the same column are given the means of the displacement parameters from $h0l$ and $h1l$, which, from the above argument, should be better than either separately.

Three-dimensional refinement

With the best parameters obtained from previous work giving a trial structure, three-dimensional refinement of all layers $h0l$ to $h3l$ was carried out in two ways: (i) by differential Fourier synthesis, with separate isotropic temperature factors for the different atoms, (ii) by a full-matrix least-squares program, with anisotropic temperature factors. Scaling had to be done by com-

parison of $\Sigma|F_{obs}|$ with $\Sigma|F_{calc}|$ for each layer separately, because of the lack of photographs about any other axis than y; this means that no reliable values could be expected for anisotropic thermal parameters along y, and though they were evaluated they are not reported. Neither refinement converged as well as would have been expected in the absence of this scaling problem, oscillations of certain parameters in successive cycles of the least-squares method being rather marked. This limited the precision of the results, but they nevertheless confirmed those from the combined *h*0*l*/*h*1*l* projections and improved on them for some parameters. In the final stages, attention was concentrated on the least-squares work, and it became clear that the oscillations were confined between narrower and recognizable limits, set out in Table 2, column 5. The final R was 9·7%.

Atomic parameters and their accuracy

The final values are those in the last column of Table 2; they are the rounded-off means of the ranges in column (5).

There are three ways of estimating the errors: (*a*) by the statistical method incorporated in the least-squares program, (*b*) as half the difference between the last two cycles of this program, and (*c*) by comparison of the separate results of the *h*0*l*/*h*1*l* work and the two three-dimensional refinements. Obviously in a case like this the conditions which would allow us to rely uncritically on (*a*) are not satisfied. Since a least-squares analysis is based on the assumption of linear relations between parameters and F's over the whole range of parameters admitted into the analysis, and since this assumption is emphatically not true when the displacement parameters systematically include zero within the range, one cannot say without detailed examination how accurate the corresponding error estimates may be when the final values of the displacements are small but not zero. The actual final values obtained for the standard deviations of the position parameters are, however, reasonable; they are ±0·0007, ±0·0018, ±0·0017, ±0·0019, for z_K, z_1, z_2, and x_2 respectively.

Inspection of the least-squares results in successive cycles suggests that method (*b*) is reliable for order of magnitude. It may however underestimate the errors in parameters which do not interact much with others.

Method (*c*) is likely to overestimate the final error, as the Fourier analysis was not carried out in such detail as the least-squares work. Comparison shows that the error of the position parameters calculated by this method is never more than twice the error calculated by (*b*), which is satisfactory confirmation; for the thermal parameters, there is only order-of-magnitude agreement.

The errors finally accepted and listed in the last column of Table 2 are those given by either (*a*) or (*b*), whichever is greater, for the position parameters, and by (*b*) for the thermal parameters. They are to be treated as if they were standard deviations. All position parameters are thus known to within ±0·002 or less, and nearly all thermal parameters in the (010) plane to within ±0·2 Å² or less.

The thermal parameters are of the order of magnitude expected for oxides with semipolar bonding, none

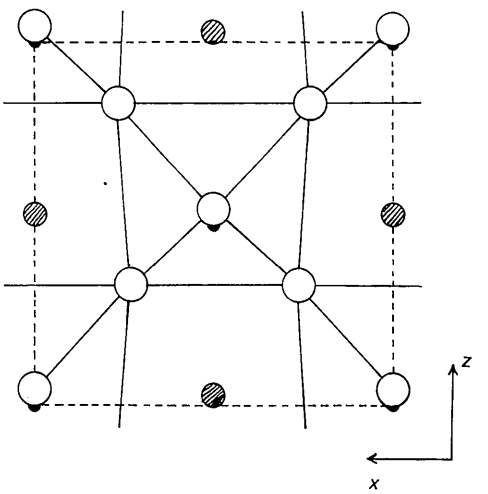

Fig. 2. Projection of structure on 010; dashed line outlines unit cell, full lines outline NbO_6 octahedra. All displacements from aristotype somewhat exaggerated.

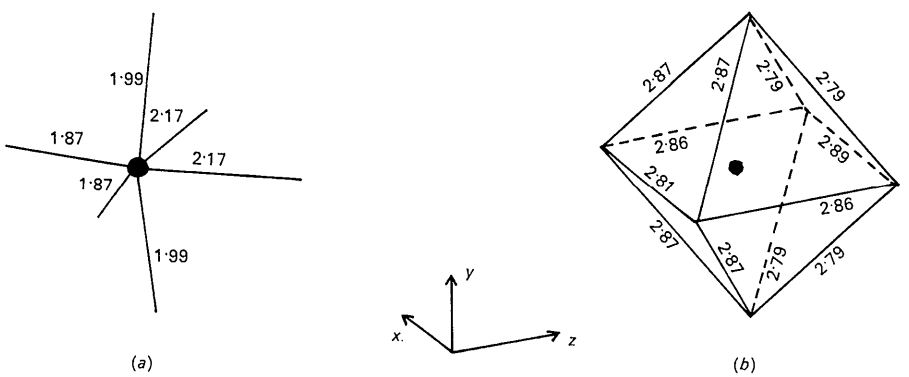

Fig. 3. Perspective diagrams of NbO_6 octahedra, showing (*a*) Nb–O bond lengths, (*b*) O–O contact distances.

being much greater than about 1·0 Å². None of the atoms show very clear thermal anisotropy, though that of O(1) is possibly real and that of O(2) more doubtfully so. For the latter, the principal values of B are 1·00 and 0·80 Å², the major axis lying at 35° to the x axis in the angle $x0\bar{z}$, *i.e.* approximately at right angles to the Nb–O bond; but the differences are too close to experimental error for the anisotropy to be significant.

Description of the structure

A projection on (010) is shown in Fig. 2, (with some of the displacements exaggerated to show their relationship). An isolated octahedron is shown in Fig. 3(*a*) and (*b*). Bond lengths and angles are listed in Table 3.

The oxygen octahedron surrounding Nb remains very nearly regular; in the (010) plane there is a difference of 0·09 Å between the long and the short edges, arising from the small x_2 parameter; while for the edges inclined to this plane, involving O(1), there is a difference of 0·10 Å between the four long ones and the four short ones, due to the difference between the z_1 and the z_2 displacements.

Within the octahedron, Nb is displaced by 0·030c, or 0·17 Å, from the centre of mass of the oxygen atoms towards the mid point of the short O(2)–O(2) edge. There are thus two long and two short Nb–O(2) bonds, the Nb–O(1) bonds being of intermediate length, but rather shorter than the mean of the other two.

The environment of K is also very regular, the extreme difference between long and short bonds being only 0·09 Å. This difference occurs between bonds inclined to the (010) plane. It is interesting to note that the tendency to equality between the two K–O(1) bonds, lying in (010), is preserved at the expense of the differences in the K–O(2) bonds and in the O(1)–O(2) edges of the octahedron.

Discussion

No very unexpected features have appeared in this structure. The most striking thing is the close resemblance to $BaTiO_3$, illustrated in Table 4. A detailed comparison of the two may therefore help to throw light on the character of the structure-building forces, and some preliminary comments will be made below.

The other point of interest is the comparative ease with which this structure was solved from visually measured intensities leading to a final R value of 10%, while tetragonal $BaTiO_3$ is notorious for the trouble it gave in spite of the extremely accurate intensity measurements (Evans, 1961). We had hoped for more favourable conditions in $KNbO_3$ because of the lower ratios of the scattering factors of the cations to those of oxygen – a condition which had allowed the solution of the structure of orthorhombic $BaTiO_3$ by neutron diffraction [Shirane, Danner & Pepinsky (1957)] – and perhaps also from the expected greater displacement of Nb. Both these factors did help. But the really important one, which might have been foreseen from the outset, had been overlooked, namely the difference in the different classes of structure factors of the aristotype due to the interchange of relative weights of the A and B cations. For $BaTiO_3$, taking the origin at Ba, the smallest class of structure factors involving the atom O(2) has the form $f_{Ba}-(f_{Ti}+f_O)$, while for $KNbO_3$, with Nb at the origin, the smallest class has the form $f_{Nb}-(f_K+3f_O)$. As noted above, it is the systematically weaker reflexions which are the best indicators of the signs of the displacements; and it was the existence of this particularly weak class in $KNbO_3$ which made an unambiguous solution of the structure possible.

The differences between orthorhombic $KNbO_3$ and orthorhombic $BaTiO_3$ can be seen from Table 4. Several points appear to be significant.

(i) The deviations from the aristotype are qualitatively alike for both materials, but their magnitude is consistently greater for $KNbO_3$, as shown by the ratios in the last column.

(ii) These systematic effects are most marked for the sheet of atoms, perpendicular to the y axis, containing Nb or Ti.

(iii) The individual values and mean values for O–O contacts are consistently greater for $KNbO_3$ than for $BaTiO_3$ in this plane; for other O–O contacts the mean

Table 3. *Bond lengths and angles*

Nb–O(1)	(2)*	1·991 ± 0·001 Å	O(2)(*s*)–Nb–O(2)(*s*)†	(1)*	97·4 ± 1·2°
Nb–O(2)	(2)	1·863 ± 0·007	O(2)(*l*)–Nb–O(2)(*l*)	(1)	83·4 ± 1·0
Nb–O(2)	(2)	2·180 ± 0·009	O(2)(*s*)–Nb–O(2)(*l*)	(2)	89·7 ± 0·5
K–O(1)	(1)	2·837 ± 0·014	O(1)–Nb–O(2)(*s*)	(4)	92·3 ± 0·6
K–O(1)	(2)	2·848 ± 0·001	O(1)–Nb–O(2)(*l*)	(4)	87·5 ± 0·6
K–O(1)	(1)	2·883 ± 0·014			
K–O(2)	(4)	2·792 ± 0·008			
K–O(2)	(4)	2·873 ± 0·010	Nb–O(1)–Nb	(1)	172·8 ± 0·7
			Nb–O(2)–Nb	(2)	168·6 ± 0·6
O(1)–O(2)	(4)	2·780 ± 0·012			
O(1)–O(2)	(4)	2·884 ± 0·012			
O(2)–O(2)	(1)	2·802 ± 0·024			
O(2)–O(2)	(1)	2·894 ± 0·024			
O(2)–O(2)	(2)	2·860 ± 0·001			

* Numbers in this column indicate numbers of equal bonds or angles per formula unit.

† For the O–Nb–O angles, the letter *s* or *l* indicates whether the Nb–O(2) bond involved is short or long.

values for the two materials are the same, though there is more scatter for $KNbO_3$.

(iv) In both materials the mean values of K–O or Ba–O bonds are equal to those of O–O, and the range of individual values is similar to that for O–O, though the detail of the scatter is different.

(v) The fact that the cell edge b is rather larger in $BaTiO_3$ than in $KNbO_3$, though the edges a and c are smaller, is not qualitatively significant, but is a consequence of the similar signs and different magnitudes of the changes of axial ratio.

Though a quantitative explanation of these effects must lie in the realm of theoretical chemistry, it is worth while trying to give a qualitative picture using rather simple concepts.

The equilibrium state of the crystal may be thought of as involving the interplay of stresses between the Nb–O, K–O, and O–O links of the framework. Con-

Table 4. *Comparison of* $KNbO_3$ *and* $BaTiO_3$ (*orthorhombic*)

Values for $BaTiO_3$ are calculated from the parameters of Shirane, Danner & Pepinsky (1957)

		$KNbO_3$	$BaTiO_3$	$BaTiO_3$:$KNbO_3$
Lattice dimensions				
	a	5·697 Å	5·669 Å	
	b	3·971	3·990	
	c	5·720	5·682	
Axial parameters				
	$c/a-1$	+0·004	+0·002	0·50
	$b/a-1$	−0·015	−0·005	0·33
Atomic parameters (relative to Nb or Ti at origin)				
	z_K or z_{Ba}	+0·017	+0·010	0·60
	z_1	+0·021	+0·020	
	z_2	+0·035	+0·023	
	x_2	+0·004	+0·003	
Parameter difference between Nb or Ti and geometrical centre of configuration of neighbouring oxygen atoms				
	Octahedron	0·030	0·022	
	Square	0·035	0·023	0·65
Displacement of Nb or Ti from geometrical centre of configuration of neighbouring oxygen atoms				
	Octahedron	0·171 Å	0·125 Å	
	Square	0·198	0·131	0·65
Bond lengths				
(i) Nb—O or Ti—O				
Short		1·86 Å	1·90 Å	
Long		2·18	2·11	
Intermediate		1·99	2·00	
Mean of long and short		2·02	2·005	
Difference of long and short		0·32	0·21	0·70
Difference of mean and intermediate		0·03	0·005	0·017
(ii) K–O or Ba—O				
In (010) plane	(1)	2·84	2·78	
	(2)	2·85	2·83	
	(1)	2·88	2·90	
	Mean	2·855	2·835	
Inclined to (010) plane	(4)	2·79	2·80	
	(4)	2·87	2·86	
	Mean	2·83	2·83	
(iii) O–O				
Octahedron edge in (010) plane	(1)	2·80	2·80	
	(2)	2·86	2·84	
	(1)	2·89	2·87	
	Mean	2·85	2·835	
Octahedron edge inclined to (010) plane	(4)	2·78	2·81	
	(4)	2·88	2·85	
	Mean	2·83	2·83	
Edge of K–O polyhedron in (010) plane		2·85	2·835	

sider first the aristotype. If NbO_6 octahedra alone contributed to the energy, the O–O links would be in a state of compression, acting as *struts*, while the O–Nb–O links would be in a state of tension, acting as *ties*. Similar conditions would hold for the KO_{12} polyhedra, if they alone contributed. Since the O–O edges are in fact common to both, and are always in compression because the interatomic force here is repulsive, the net effect of the O–Nb–O and O–K–O links must be a tensile stress; hence, since the Nb–O bonds are stronger than K–O and vary more rapidly with distance, the O–Nb–O links must be in tension, while the O–K–O links may be either in tension or in compression.

If the stress-strain relation in a link is non-linear, with greater energy differences for small decreases of length than for small increases of equal magnitude, the stress in O–Nb–O can be relieved without overall change of length by allowing Nb to move off-centre; alternatively, the length of the tie can be increased while the stress remains equal to that in the symmetrical configuration; or, more generally, there will be an increase of length combined with a decrease in tension. This argument does not inquire into the reason for the non-linear behaviour, which is in fact likely to be strongly influenced by the polarization of O by the closer approach of Nb.

In orthorhombic $KNbO_3$, the displacement of Nb is such as to reduce the tension in two O–Nb–O ties at right angles. We therefore argue as follows.

(i) The relief of O–Nb–O tension will be greatest (by analogy with the one-dimensional case) in directions where long and short Nb–O bonds alternate, *i.e.* the direction of the Nb displacement. Hence the average relief of O–O compression will be greatest in this direction. Assuming that the octahedra are not free to rotate, this will therefore be the direction of elongation of the unit cell. This prediction agrees with the experimental observation.

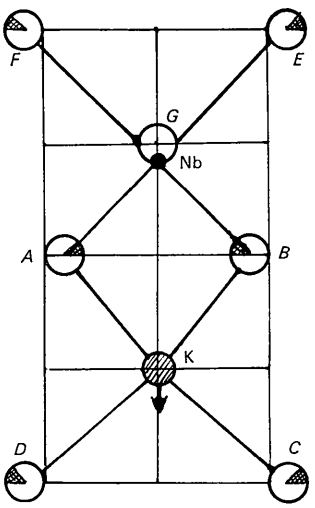

Fig. 4. Projection of part of unit cell, schematic: K and O(1) (*G*) are shown undisplaced, and Nb and O(2) (*A* to *F*) with exaggerated displacements; shaded sectors of O(2) indicate regions involved in tightly bonded Nb–O triangles.

(ii) The average relief of O–O compression in the plane of the Nb displacement will be greater than in directions inclined to it, since the O–Nb–O ties perpendicular to this plane retain the length appropriate to a symmetrical configuration. The average length of O(2)–O(2) edges will therefore be greater than of O(2)–O(1) edges. The truth of this prediction can be seen from Table 4, where the lengths are 2·85 and 2·83 Å respectively.

(iii) The argument in (ii) neglects the effect in the aristotype of stresses in K–O; as explained above, compression in K–O will enhance the effect, tension in K–O will diminish it. The rather large differences observed between the two kinds of O–O edges argue for compression in K–O.

(iv) The condition that the octahedra are not free to take up positions tilted relative to one another is imposed by the length of the K–O bond. Any substantial tilting would produce intolerable compressions in some of the O–K–O struts. This is a restatement of the familiar idea that packing requirements of K are the effective cause maintaining the parallel orientation of the octahedra.

Comparison of $BaTiO_3$ with $KNbO_3$ shows that the effects are closely similar but smaller in magnitude. Hence, in the aristotype, either the tension in O–Ti–O or the compression in O–Ba–O, or both, must be less than in O–Nb–O or O–K–O respectively.

The only deviation from the aristotype which is greater for $BaTiO_3$ than for $KNbO_3$ is the off-centring of Ba in its quadrilateral of neighbouring O(1)'s. To understand the implications of this, it is instructive to consider its development as the consequence of a sequence of other displacements. Fig. 4 illustrates it for $KNbO_3$. Starting with the aristotype, the first step is the displacement of Nb to form strong bonds with the two O(2)'s marked *A* and *B*. The two latter approach one another, forming a rather tightly bound triangle with the Nb. If K remains unmoved, the bonds K*A* and K*B* will be slightly shortened, K*C* and K*D* slightly lengthened. But this is wrong from the point of view of the electronic charge distribution within *A*, *B*, *C*, and *D*, *i.e.* of their polarization. On the sides of *A* and *B* facing K, the electron cloud is more closely involved in the binding of the NbO_2 triangle, whereas on the sides of *C* and *D* facing K it is freer of this. Hence one may expect a displacement of K in the direction shown, to shorten K*C* and K*D* and lengthen K*A* and K*B*. But this will put it off-centre in its quadrilateral of neighbouring O(1)'s, the bond KG being now anomalously short. To equalize the K–O(1) bonds, O(1)(*G*) must move in the same direction. In so doing, it distorts the regularity of the octahedron. The position finally adopted is such as to make the sum of the energies associated respectively with the K–O(1) distortions and the distortion of the octahedron a minimum.

The difference between the balance points achieved by $KNbO_3$ and $BaTiO_3$ is apparent from Table 4. Both substances have the same differences between long and short K–O(2) or Ba–O(2) bonds (K*A* and K*C* of Fig. 4). For $BaTiO_3$, however, the difference between long and short Ba–O(1) bonds is 0·12 Å, and between long and short O(1)–O(2) edges is 0·04 Å, while for $KNbO_3$ the relative magnitudes are roughly interchanged, being 0·04 Å and 0·10 Å respectively. This supports the earlier suggestion that the K–O(1) links are already in compression and resistant to further compression. By contrast, either Ba is intrinsically smaller than K or it is more capable of polarizing the O atom to give unequal bonds; again, both causes may cooperate in the observed effect.

We put forward this qualitative treatment in the hope that it may direct attention to aspects of the structures where more rigorous treatment might lead to very profitable results.

We wish to express our indebtedness to Dr R. Ueda for his collaboration in the first part of the work. One of us (L.K.) is grateful for a National Science Foundation Science Faculty Fellowship.

References

DAUBEN, C. H. & TEMPLETON, D. H. (1955). *Acta Cryst.* **8**, 841.
EVANS, H. T. (1961). *Acta Cryst.* **14**, 1019.
FARQUHAR, M. G. M. & LIPSON, H. (1946). *Proc. Phys. Soc.* **58**, 200.
FORSYTH, J. B. & WELLS, M. (1959). *Acta Cryst.* **12**, 412.
GELLER, S. (1961). *Acta Cryst.* **14**, 1026.
MEGAW, H. D. (1962). *Acta Cryst.* **15**, 972.
SHIRANE, G., DANNER, H. & PEPINSKY, R. (1957). *Phys. Rev.* **105**, 856.
SHIRANE, G., NEWNHAM, R. E. & PEPINSKY, R. (1954). *Phys. Rev.* **96**, 581.
THOMAS, L. H. & UMEDA, K. (1957). *J. Chem. Phys.* **26**, 293.
VOUSDEN, P. (1951). *Acta Cryst.* **4**, 375.
WOOD, E. A. (1951). *Acta Cryst.* **4**, 353.

Acta Cryst. (1967). **22**, 648

The Crystal Structure of α-L-Sorbose

BY S. H. KIM AND R. D. ROSENSTEIN
Crystallography Laboratory, University of Pittsburgh, Pittsburgh, Pa. 15213, *U.S.A.*

(*Received* 25 *July* 1966)

The crystal structure of L-sorbose $C_6H_{12}O_6$ has been determined from the three-dimensional sharpened Patterson function by superposition and convolution methods on an IBM 1620 computer. Both photographic and automatic diffractometer data were measured. The former gave a final R index of 8·1 % and the latter 5·1 %. The space group is $P2_12_12_1$ with four molecules in a unit cell of dimensions a = 6·535 (σ = 0·004), b = 18·069 (σ = 0·007), c = 6·305 (σ = 0·004) Å. The molecules are the α-anomer of the pyranose form. They are associated in the crystal by extensive hydrogen-bonding, which includes all the hydroxyl groups and the ring oxygen atom. The primary alcohol group is disordered, and this leads to an apparent shortening of corresponding C–OH bonds. With the exception of these bonds, the C–C and C–O distances do not differ significantly from the mean values of 1·516 and 1·424 Å respectively.

Introduction

L-Sorbose ($C_6H_{12}O_6$, also called sorbinose) is found in the enzyme hydrolyzate of certain pectins. It is believed to exist in both the ketohexose (I) and the pyranose (II) forms.

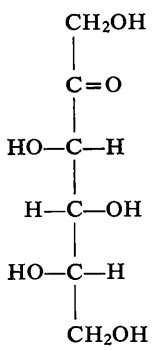

(I)

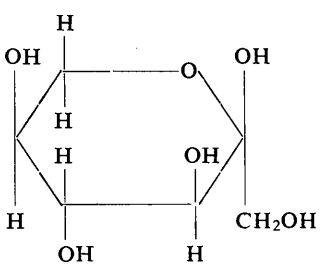

(II)

As an important intermediate in the commercial synthesis of ascorbic acid, it is most conveniently obtained by the biochemical oxidation of sorbitol (Bertrand, 1898; Wells, Stubbs, Lockwood & Roe, 1937). Hudson (1925) suggested, on the basis of the calculation of the specific rotation, that the common form is the α-anomer of the pyranose (II) which is confirmed by this work. The conventional numbering of the carbon and oxygen atoms used in this paper is shown in Fig. 1.

Crystal data

Large transparent crystals were obtained by slow evaporation of an aqueous solution of the compound supplied by Pfanstiehl Laboratories, Inc. The cell parameters were measured at 22 °C with Cu $K\alpha_1$ and Cu $K\alpha_2$ radiation using a Picker 4-angle automatic diffractometer. The crystal density was measured by flotation in a liquid mixture of carbon tetrachloride, chloroform and bromoform.